

# Dual hollow core fiber-based Fabry–Perot interferometer for measuring the thermo-optic coefficients of liquids

Cheng-Ling Lee,\* Hsuan-Yu Ho, Jheng-Hong Gu, Tung-Yuan Yeh, and Chung-Hao Tseng

Department of Electro-Optical Engineering, National United University, Miaoli 360, Taiwan

\*Corresponding author: cherry@nuu.edu.tw

Received October 31, 2014; revised December 15, 2014; accepted December 26, 2014;

posted January 7, 2015 (Doc. ID 226083); published February 4, 2015

A microcavity fiber Fabry–Perot interferometer (MFFPI) that is based on dual hollow core fibers (HCFs) is developed for measuring the thermo-optic coefficients (TOCs) of liquids. The proposed MFFPI was fabricated by fusion-splicing a tiny segment of the main-HCF with a diameter  $D$  of 30  $\mu\text{m}$  and another section of feeding-HCF with a diameter of 5  $\mu\text{m}$ . Then, the main-HCF was filled with liquid by capillary action through the feeding-HCF by immersing the MFFPI in the liquid. The TOCs of the Cargille liquid ( $n_D = 1.3$ ), deionized (DI) water, and ethanol were accurately determined from the shift of the interference wavelength, which was due to the temperature variation. Our experimental results were also compared with other published studies to investigate the effectiveness of the proposed sensing scheme. The major advantage is that the miniature MFFPI can achieve the measurement of the TOCs of the liquids with picoliter volume, and the measured liquids also can be sealed off and stored inside the HCF to prevent contamination. © 2015 Optical Society of America

OCIS codes: (060.2370) Fiber optics sensors; (060.2340) Fiber optics components; (120.2230) Fabry-Perot; (120.4530) Optical constants; (280.4788) Optical sensing and sensors.

<http://dx.doi.org/10.1364/OL.40.000459>

The measurement of the optical constants (OCs) of a material is essential in the fields of optics and optoelectronics. One important OC, the thermo-optic coefficient (TOC), has been extensively investigated to evaluate the thermal variation of the refractive index (RI) of materials. The simplest expression of the TOC is derivative of the RI  $n$  with respect to the temperature  $T$  at a wavelength ( $\lambda$ ) of  $dn(\lambda)/dT$ . Some fiber-based sensors simultaneously measure the RI and temperature of materials [1–8]. Information about the variations in temperature and the RI enable the TOCs of measured liquids to be readily obtained [5,6]. Thus, the in-line liquid-core fiber Fabry–Perot interferometer (FFPI) is an excellent candidate device for easily and accurately measuring the TOC of liquids. Various FFPIs with smart, simple, and hybrid structures have a wide range of applications in the parametric sensing of different elements, such as of ambient temperature [9–11], the external RI [12,13], strain [14], and other properties [15]. Regardless of whether FFPIs are fabricated by splicing various fibers, chemical etching, or by femtosecond laser machining, they can achieve the well-known two-beams interference mechanism and exhibit low-finesse Fabry–Perot (FP) interferometric characteristics. Excluding the above configurations of the FFPIs, a liquid-filled microcavity hollow core fiber (HCF) with a miniature cavity that is filled with various liquids can be used to measure some physical and optical parameters of micro-specimens of liquids. Accordingly, to the best of the authors' knowledge, this work is the first to present a liquid core fiber sensor for measuring the TOCs of liquids. The studied device is based on a microcavity fiber Fabry–Perot interferometer (MFFPI), which is composed of two tiny sections of fusion-spliced HCFs with different core diameters to achieve FP interference. The interferometer fabricated by fusion splicing a small segment of main-HCF (named as HCF<sub>1</sub>) with a diameter  $D$  of 30  $\mu\text{m}$  with a single-mode

fiber (SMF). The endface of HCF<sub>1</sub> was fusion-spliced with another segment of a feeding-HCF (HCF<sub>2</sub>) with  $D = 5 \mu\text{m}$ . After the splicing of the HCF<sub>2</sub>, its endface was cleaved with a slant to prevent the undesired Fresnel reflection from the fiber/air interface. The insertion loss of the device averages 0.05 dB per micrometer of HCF length. Thereafter, HCF<sub>1</sub> was filled with test liquids by capillary action through HCF<sub>2</sub>. This was achieved by immersing the ends of HCF<sub>2</sub> into each liquid. Figure 1 shows the microphotograph of the MFFPI sensor tip for measuring the TOCs of liquids. According to the experimental results, the developed MFFPI can accurately measure the TOC of volumes of liquids, the values of which are in picoliters.

After the sensor has been fabricated, it is dipped in liquid samples, the temperatures of which were controlled by using a TE cooler (resolution: 0.05°C). When a wideband light source is incident to the device, the two reflective beams from the liquid/silica interfaces of the main microcavity HCF<sub>1</sub> are combined in the SMF, producing interference patterns. Light that propagates into the HCF<sub>2</sub> section in which  $D = 5 \mu\text{m}$  cannot cause FP interference. It can only excite some leaky modes, thereby increasing the loss associated with the reflection. The main FP interference that is obtained by HCF<sub>1</sub> can be

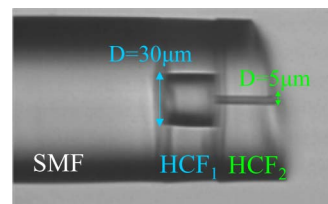


Fig. 1. Microphotograph of the MFFPI sensor tip. Here, HCF<sub>1</sub> has a diameter of 30  $\mu\text{m}$ , and HCF<sub>2</sub> has a diameter of 5  $\mu\text{m}$ . The cavity length of the HCF<sub>1</sub> herein is about 33.84  $\mu\text{m}$ .

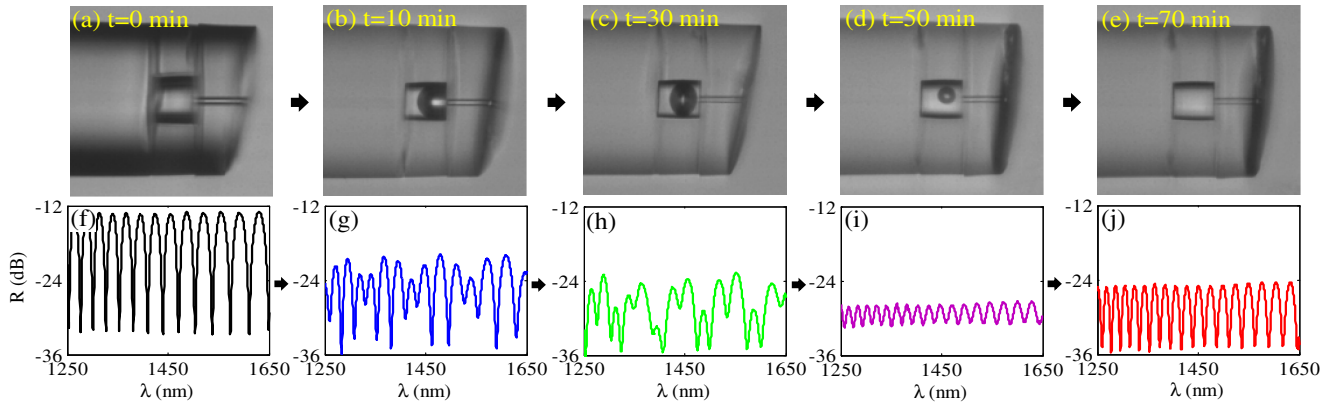


Fig. 2. (a)–(e) Microphotographs of the evolution of liquid being poured into the proposed MFFPI sensor with DI water. (f)–(j) The corresponding spectra of the conditions of (a)–(e), respectively.

observed, and the interference spectra are readily analyzed using an optical spectrum analyzer (OSA).

In the experiment, HCF<sub>1</sub> was filled with the standard Cargille optical liquid for which  $n_D = 1.3$ , ethanol, for which the value of  $n_D$  is 1.361, and deionized (DI) water in which  $n_D = 1.333$  through HCF<sub>2</sub> to determine their TOCs by the proposed sensing scheme. The value of  $n_D = 1.3$  is the RI measured at 25°C, at the Sodium D Line, at 589.3 nm. To ensure that the liquid filled the main microcavity of HCF<sub>1</sub>, the evolution of the DI water filling the microcavity by capillary action was monitored under a microscope, as shown in Figs. 2(a)–2(e). As presented in these figures, the DI water gradually filled the microcavity of HCF<sub>1</sub> via HCF<sub>2</sub> until all of the residual air was eliminated. The corresponding reflective spectra were simultaneously recorded using the OSA, and are displayed in Figs. 2(f)–2(j). The partially filled microcavity forms multiple cavities that produce combined interference patterns [see Figs. 2(g) and 2(h)]. Once HCF<sub>1</sub> has been completely filled with liquid, the optical spectra do not change. In this case, the duration of the capillary action takes less than 70 min. The volume of the liquid in HCF<sub>1</sub> is estimated to be approximately 25 pl. At this moment of complete filling, two Fresnel beams from the liquid/silica interfaces of the main cavity HCF<sub>1</sub> can achieve the pure sinusoidal FP interference [Fig. 2(j)]. Figure 3 shows the

pure sinusoidal interference spectra of the MFFPIs with the micro-cavity that was completely filled with air, Cargille liquid, DI water, and ethanol. The wideband interference spectra of the liquid-filled MFFPIs yield the RI that corresponds to the wavelength  $\lambda$  in the liquid. The relationship between the RI and  $\lambda$  is easily determined using the following equation:

$$n(\lambda) = \frac{\lambda_1 \lambda_2}{2d(\lambda_2 - \lambda_1)}, \quad (1)$$

where  $n$  is the RI at a wavelength of  $\lambda$  where  $\lambda^2 \sim \lambda_1 \lambda_2$ , and  $\lambda_1$  and  $\lambda_2$  represent the wavelengths of the two adjacent interference peaks in the interference spectra.

In the TOC measurement, the temperature  $T$  of the liquid-filled MFFPI was increased from 20°C to 60°C to evaluate the effect of  $T$  on the interference spectra. When the proposed sensor was heated, the interference spectra shifted to shorter wavelengths (blueshifted). Figures 4(a)–4(c) display the wavelength shift of the interference peaks/dips as  $T$  is increased from 20°C to 60°C for (a) the Cargille liquid ( $n_D = 1.3$ ), (b) the DI water ( $n_D = 1.333$ ), and (c) ethanol ( $n_D = 1.361$ ), respectively. The insets of Figs. 4(a)–4(c) display the detailed wavelength shift ( $\Delta\lambda$ ) due to the thermal effect on the RI of the liquids. The wavelength is blueshifted, and the peak intensity is very slightly increased as the RI decreases and  $T$  increases. The measured sensitivity ( $\Delta\lambda/\Delta T$ ) is very linear from 20°C to 60°C. A larger slope of  $\Delta\lambda$  as a function of  $T$  corresponds to a higher estimated TOC.

Based on the experimental results in Fig. 4, the TOC of the liquids can be obtained by analyzing the shifts in the interference dips/peaks. Figure 5 schematically depicts the shift of the interference spectra of the liquid MFFPI as  $T$  increases.  $\lambda$  and  $\lambda'$  corresponds to the interference dips at  $T$  and  $T' = T + \Delta T$ , respectively.

Here, the wavelength shift is defined as  $\Delta\lambda \equiv \lambda' - \lambda$  and the two wavelengths of the dips  $\lambda'$  and  $\lambda$  are satisfied by the following relationship:

$$\frac{2nd}{\lambda} = \frac{2n'd'}{\lambda'}. \quad (2)$$

Here,  $n$  and  $n'$  are the RIs of the liquid at  $T$  and  $T'$ , respectively;  $d$  and  $d'$  are the lengths of the

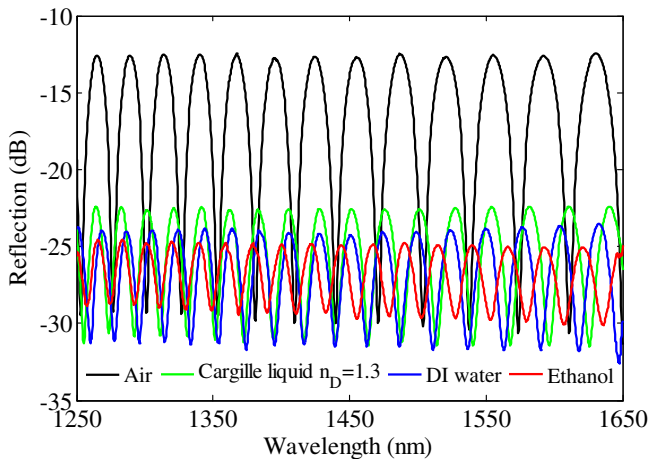


Fig. 3. Reflective spectra of proposed MFFPI filled with air, Cargille liquid ( $n_D = 1.3$ ), DI water, and ethanol, when  $T = 20^\circ\text{C}$ .

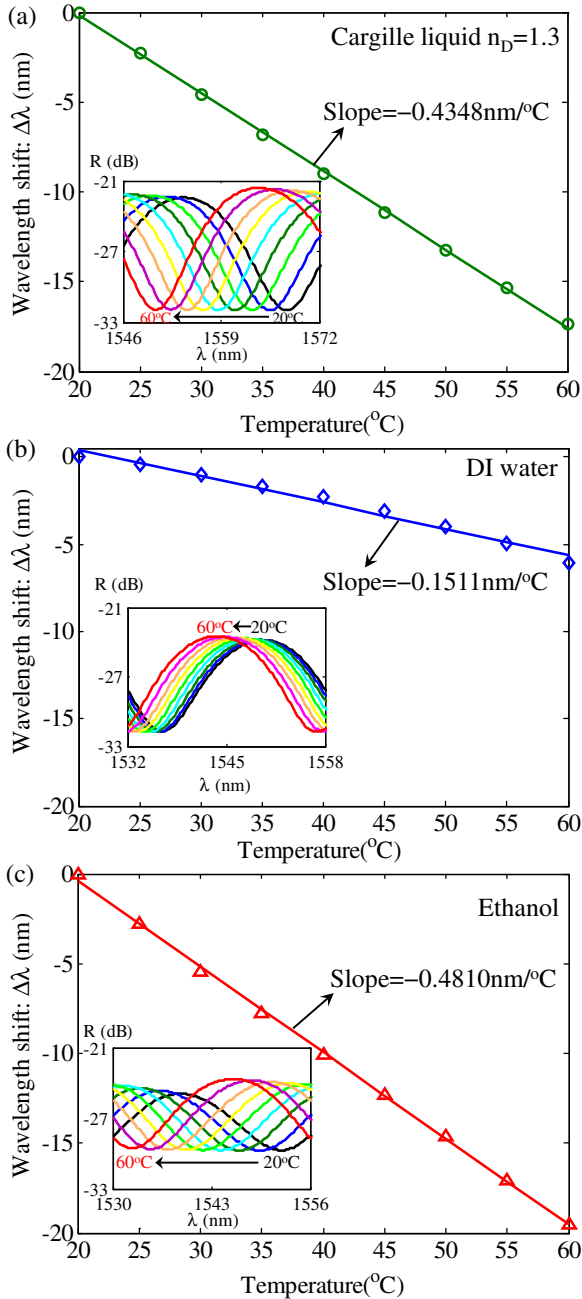


Fig. 4. Sensitivity of the wavelength shift in temperature from 20°C to 60°C for (a) the Cargille liquid where  $n_D = 1.3$ , (b) the DI water, and (c) the ethanol. Insets show corresponding spectra with an increasing  $T$ .

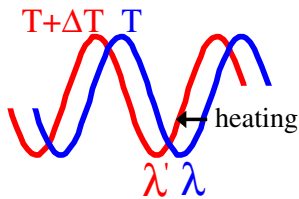


Fig. 5. Schematic shift of the interference spectrum as  $T$  changes to  $T' = T + \Delta T$ .

microcavity at  $T$  and  $T'$ , respectively.  $\Delta d = d' - d$  is the increase of the cavity due to its thermal expansion. Therefore, Eq. (2) is rearranged as follows:

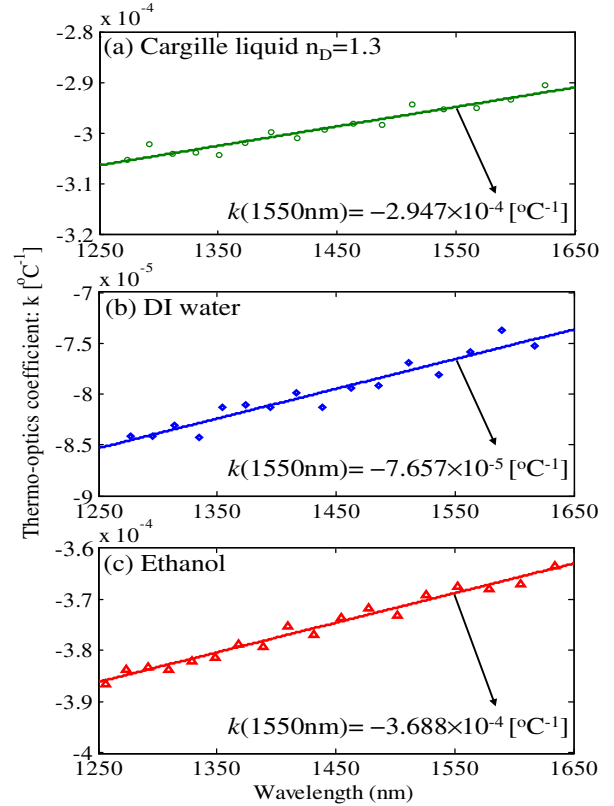


Fig. 6. Obtained TOCs that correspond to  $\lambda$  of the Cargille liquid ( $n_D = 1.3$ ), the DI water ( $n_D = 1.333$ ), and the ethanol ( $n_D = 1.336$ ). The arrows indicate the TOC values at  $\lambda = 1550$  nm.

$$\frac{nd}{\lambda} = \frac{(n + nk\Delta T)(d + \alpha\Delta T)}{\lambda'}, \quad (3)$$

where  $\alpha$  is the thermal expansion coefficient of silica ( $\sim 5.5 \times 10^{-6} \text{ } ^\circ\text{C}^{-1}$ ) and  $k$  represents the TOC of the filled liquid. The  $k(\lambda)$  can be calculated using

$$k(\lambda) = \frac{\frac{\lambda'}{\lambda} - \alpha\Delta T - 1}{\Delta T + \alpha\Delta T^2}. \quad (4)$$

Figures 6(a)–6(c) show the obtained value of  $k(\lambda)$  for the test liquids: the Cargille liquid, the DI water, and the ethanol, respectively. The values are calculated by Eq. (4) and based on the experimental results in Fig. 4. Figure 6 indicates that the measured TOCs are slightly correlated with the operation  $\lambda$ . The results for the different liquids reveal that the TOCs increase slightly with  $\lambda$ . The determined TOCs ( $k$ ) are further compared with those in the literatures [5–7] and are found to agree closely. The  $k(\lambda)$  of the DI water and the ethanol at  $\lambda = 1550$  nm are  $-7.657 \times 10^{-5}$  (published data:  $-9.646 \times 10^{-5}$  in [5] and  $-8.00 \times 10^{-5}$  in [7]) and  $-3.688 \times 10^{-4}$  (published data:  $-3.140 \times 10^{-4}$  in [5] and  $-3.99 \times 10^{-4}$  in [6]), respectively. The measured  $k(\lambda)$  of the Cargille liquid ( $n_D = 1.3$ ) at  $\lambda = 1550$  nm has not yet been found in the literature. Thus, the determined value of  $-2.947 \times 10^{-4}$  (at  $\lambda = 1550$  nm) by our MFFPI is merely compared with the reference data of  $-3.32 \times 10^{-4}$  (at  $\lambda = 589.3$  nm) from the

**Table 1. Comparisons of the Measured TOCs of the Liquids used Between the Results of our Sensor and That of the Published Work of [5–7] and [16]**

Liquids	Cargille-liquid $n_D = 1.3$	DI Water $n_D = 1.333$	Ethanol $n_D = 1.361$
TOC: $k$ [ $^{\circ}\text{C}^{-1}$ ] (measured in the study)	$-2.947 \times 10^{-4}$ (at $\lambda = 1550$ nm)	$-7.657 \times 10^{-5}$ (at $\lambda = 1550$ nm)	$-3.688 \times 10^{-4}$ (at $\lambda = 1550$ nm)
TOC: $k$ [ $^{\circ}\text{C}^{-1}$ ] (published data)	$-3.32 \times 10^{-4}$ [16] (at $\lambda = 589.3$ nm)	$-9.646 \times 10^{-5}$ [5] (at $\lambda = 1550$ nm) $-8.00 \times 10^{-5}$ [7] (at $\lambda = 1550$ nm)	$-3.140 \times 10^{-4}$ [5] (at $\lambda = 1550$ nm) $-3.99 \times 10^{-4}$ [6] (at $\lambda = 1550$ nm)

Cargille Labs [16]. The comparisons are arranged and shown in Table 1.

In conclusion, this work has developed and demonstrated a dual HCF Fabry–Perot interferometer that can effectively and accurately determine the TOC of liquids in picoliter volumes. Experimental results demonstrate that the measured values deviate only by  $10^{-5}$ – $10^{-6}$  from published results for the same liquids. The proposed liquid-filled MFFPI also has the advantage of being able to determine the dispersion of the RI of a picoliter-volume solution. We believe that the proposed ultra-compact all-fiber sensor with a linear response is highly suitable for measuring the TOCs of micro-specimens in the biomedical and biochemical fields.

The authors would like to thank the National Science Council of the Republic of China, Taiwan, for financially supporting this research under Contract No. NSC 102-2221-E-239-033-MY3.

## References

1. T. Zhu, Y. J. Rao, and Q. J. Mo, *IEEE Photon. Technol. Lett.* **17**, 2700 (2005).
2. D. A. C. Enríquez, A. R. da Cruz, and M. T. M. R. Giraldo, *Opt. Laser Technol.* **44**, 981 (2012).
3. S. M. Lee, S. S. Saini, and M. Y. Jeong, *IEEE Photon. Technol. Lett.* **22**, 1431 (2010).
4. X. Chen, K. Zhou, L. Zhang, and I. Bennion, *Appl. Opt.* **44**, 178 (2005).
5. Y. H. Kim, S. J. Park, S. W. Jeon, S. Ju, C. S. Park, W. T. Han, and B. H. Lee, *Opt. Express* **20**, 23744 (2012).
6. R. C. Kamikawachi, I. Abe, A. S. Paterno, H. J. Kalinowski, M. Muller, J. L. Pinto, and J. L. Fabris, *Opt. Commun.* **281**, 621 (2008).
7. A. N. Chryssis, S. S. Saini, S. M. Lee, and M. Dagenais, *IEEE Photon. Technol. Lett.* **18**, 178 (2006).
8. C. B. Kim and C. B. Su, *Meas. Sci. Technol.* **15**, 1683 (2004).
9. C. L. Lee, L. H. Lee, H. E. Hwang, and J. M. Hsu, *IEEE Photon. Technol. Lett.* **24**, 149 (2012).
10. C. L. Lee, C. H. Hung, C. M. Li, and Y. W. You, *Opt. Commun.* **285**, 4395 (2012).
11. C. L. Lee, H. J. Chang, Y. W. You, G. H. Chen, J. M. Hsu, and J.-S. Horng, *IEEE Photon. Technol. Lett.* **26**, 749 (2014).
12. Y. J. Rao, M. Deng, D. W. Duan, X. C. Yang, T. Zhu, and G. H. Cheng, *Opt. Express* **15**, 14123 (2007).
13. C. L. Lee, J. M. Hsu, J. S. Horng, W. Y. Sung, and C. M. Li, *IEEE Photon. Technol. Lett.* **25**, 833 (2013).
14. F. C. Favero, L. Araujo, G. Bouwmans, V. Finazzi, J. Villatoro, and V. Pruneri, *Opt. Express* **20**, 7112 (2012).
15. C. L. Lee, Y. C. Zheng, C. L. Ma, H. J. Chang, and C. F. Lee, *Appl. Phys. Lett.* **102**, 193504 (2013).
16. <http://www.cargille.com/msds.shtml>.